Complete tight-binding description of the empirical-local-pseudopotential Hamiltonian in zinc-blende semiconductors

D. S. Tang
Department of Physics and Microelectronics Research Center, The University of Texas at Austin, Austin, Texas 78712-1081
(Received 11 April 1988)

A complete spatial description of the empirical-local-pseudopotential Hamiltonian in zinc-blende–structure semiconductor materials based on the tight-binding theory is presented. The sp^3 Gaussian orbitals are employed to construct the Bloch basis functions which are subsequently used in obtaining the Hamiltonian matrix. The spatial correlation of the neighbor quasiatomic wave functions is estimated. It is shown that to produce an energy-band structure comparable to that of the plane-wave basis, a cluster of at least 135 primitive cells is required. The intermediate-range interactions are important in determining the dispersion of the band structure. We evaluated the GaAs energy band as an illustration.

I. INTRODUCTION

The tight-binding model[1] is a numerically straightforward and physically appealing approach to the study of the properties of the electronic band structure of semiconductor materials. Physically, a bulk material is a congregation of an order of 10^{23} atoms which behave hydrogen-atom-like when isolated. When these atoms are brought close together, the atomic wave functions overlap and form bonding and antibonding orbitals which constitute the valence and conduction bands of the material. It is therefore natural to construct the Bloch basis functions as a linear superposition of the atomiclike wave functions in accordance with the Bloch's theorem. However, it is well known[2] that when the nearest-neighbor interaction is used to develop the single-particle Hamiltonian, the tight-binding theory fails to produce the correct conduction-band structure of many materials. Extension to the next- and higher-order–nearest-neighbor interactions is simple in principle, but it suffers from the drawback that too many adjustable parameters are involved to fit the experimental band structure. As a consequence, it loses its simplicity and becomes impractical. A simple way[3,4] to handle the band-structure calculation up to eight nearest neighbors is to employ the Hartree-Fock effective one-electron operator and to set the ionization energies of the s and p orbitals to their atomic values. Then the dimensionless empirically adjustable parameters[3] K_{ss} and K_{pp} for the s-s interaction and the p-p interaction, respectively, in this extended Hückel theory are chosen to be 1.75. The K_{sp} parameter for the s-p interaction and the s- and p-orbital exponents are subsequently adjusted to produce the best fit. However, this approach[4] produces $E(X_{1c})=3.79$ eV in GaAs, 1.76 eV higher than that in empirical-nonlocal-pseudopotential method. Attempts[5] to improve the nearest-neighbor tight-binding theory by including an excited S^* state in addition to the sp^3 basis per atom produce results which are still unsatisfactory in producing a flatter first-conduction-band dispersion when compared with the empirical-nonlocal-pseudopotential band structure. Earlier, Chadi[6] proposed to apply the localized orbitals to the local-pseudopotential in the momentum space and successfully produced the bulk band structures comparable to that evaluated in the plane-wave basis. This idea was further extended by Chen and Sher[7] in their study of the energy band of the random alloy and of orthonormal local orbitals in III-V compound semiconductors. Based on a set of nonorthonormal local orbitals, Chen and Sher used a **k**-space construction procedure to produce a set of orthonormal local orbitals through Löwdin's diagonalization process. Bloch functions are then represented through these orthonormal local orbitals and the Hamiltonian matrix elements are subsequently constructed. Numerical calculation demonstrated that extended interactions up to the fifteenth-shell neighbors are needed to be included to account for the valence and conduction bands. These results are in qualitative agreement with our results to be reported in this paper in which a direct approach is employed. This paper reports another aspect of the tight-binding theory applied to the local-pseudopotential Hamiltonian; namely, the spatial behavior of the wave-function correlation and intermediate-range interactions of the local-pseudopotential Hamiltonian. The analysis is carried out in the coordinate space and therefore brings out the physical nature of the tight-binding theory. In doing so, a deeper insight to the underlying physical principles governing the formation of bulk band structure can be gained. Furthermore, the techniques and results to be presented in this paper are relevant to the study of defects, heterojunctions, and microstructures. A nonempirical tight-binding method which takes the interactions with many neighbors into account has been proposed by Lafon and Lin[8] and subsequently applied to diamond, silicon, and sodium crystals by Chaney *et al.*,[8] Kane,[9] and Ciraci and Batra.[10] These first-principles self-consistent techniques use a variety of schemes to construct the core potential and the exchange potential. These have demonstrated that the linear combination of Gaussian orbitals method simplifies the computational procedure. However, Wang and Klein[11] reported that this self-consistent

linear combination of Gaussian orbitals method applied to the local-density theory for band-structure calculation underestimates the optical band gaps by 30% or more. This has been attributed to the partial failure of the local-density theory in describing excited states. Therefore, for the sake of practicality and simplicity in the application of band-structure calculation to microelectronics, the empirical-pseudopotential method remains one of the versatile schemes to use. In going into a tight-binding description, a further computational advantage is gained in that one diagonalizes an 8×8 Hamiltonian matrix in the minimum basis set of s, p_x, p_y, and p_z orbitals, instead of an 89×89 (or larger) Hamiltonian matrix in the plane-wave basis. We organize the presentation in the following manner. Section II is on the general formalism of the tight-binding theory in relation to the local-pseudopotential Hamiltonian. Spatial properties of the Hamiltonian will be analyzed in Sec. III. The spatial correlation factor of the neighboring atomic wave functions are explicitly defined and estimated. We evaluated the band structure of GaAs as an illustration and the numerical results are presented in Sec. IV. Section V is the conclusion.

II. TIGHT-BINDING FORMALISM

To introduce notations for the discussion below, we briefly review Chadi's tight-binding approach.[6] The Bloch basis function $\phi_\alpha^{(i)}(\mathbf{k},\mathbf{r})$ for a given crystal momentum $\mathbf{k}$ is constructed as a linear superposition of the atomic wave functions centered around each of the atomic site of the crystal lattice:

$$\phi_\alpha^{(i)}(\mathbf{k},\mathbf{r})=\sum_{\mathbf{R}} e^{\mathbf{k}\cdot\mathbf{R}} f_\alpha(\mathbf{r}-\mathbf{R}-\tau_i)\ . \tag{1}$$

$\mathbf{R}$ is the lattice vector of a primitive cell containing a cation at τ_1 and an anion at τ_2 ($i=1$ or 2 for anion and cation, respectively). The displacement vector τ_i is measured with respect to $\mathbf{R}$. α denotes the orbital label. In the minimum basis set, α means the s, p_x, p_y, or p_z orbital. We use the Gaussian orbitals in our study. They are $f_s(\mathbf{r})=C_s e^{-\lambda_i r^2}$, $f_{p_x}=C_{P_x} x e^{-\lambda_i r^2}$, $f_{p_y}=C_{p_y} y e^{-\lambda_i r^2}$, and $f_{pz}=C_{p_z} z e^{-\lambda_i r^2}$, respectively. Here, the explicit form of the normalization constants C_s, C_{p_x}, C_{p_y}, and C_{p_z} which are functions of the variational parameter λ_i are not important as they are easily evaluated numerically when the Bloch basis functions are properly normalized in the computer code. In general, the Bloch basis functions are nonorthogonal and the overlap integrals are formally

$$S_{\alpha\beta}^{ij}(\mathbf{k})=\langle \phi_\alpha^{(i)}(\mathbf{k},\mathbf{r})|\phi_\beta^{(j)}(\mathbf{k},\mathbf{r})\rangle\ , \tag{2}$$

and similarly, the matrix elements of the Hamiltonian H are given by

$$H_{\alpha\beta}^{ij}(\mathbf{k})=\langle \phi_\alpha^{(i)}(\mathbf{k},\mathbf{r})|H|\phi_\beta^{(j)}(\mathbf{k},\mathbf{r})\rangle \tag{3}$$

which constitutes an 8×8 Hamiltonian matrix in the minimum basis set. To proceed further without invoking the momentum representation as Chadi did, we need to employ the following property of the matrix element of a general bounded spatial periodic function $G(\mathbf{r})=G(\mathbf{r}+\mathbf{R})$:

$$\langle \phi_\alpha^{(i)}(\mathbf{k},\mathbf{r})|G(\mathbf{r})|\phi_\beta^{(j)}(\mathbf{k},\mathbf{r})\rangle=N\sum_{\mathbf{R}} e^{\mathbf{k}\cdot\mathbf{R}} g_{\alpha\beta}^{ij}(\mathbf{R}) \tag{4a}$$

with

$$g_{\alpha\beta}^{ij}(\mathbf{R})\equiv\int d\mathbf{r}\, f_\alpha(\mathbf{r}-\tau_i)G(\mathbf{r})f_\beta(\mathbf{r}-\mathbf{R}-\tau_j)\ . \tag{4b}$$

Here, N is the number of lattice sites in the crystal. The above equality is a consequence of the translational invariance of the summation over $\mathbf{R}$ and of the integration over $\mathbf{r}$. The integration over $\mathbf{r}$ is throughout the crystal volume. The physical implication of Eq. (4a) is almost explicit; namely, each lattice site $\mathbf{R}$ contributes to the matrix element by an amount equal to the g function $g_{\alpha\beta}^{ij}(\mathbf{R})$ (e.g., the overlap integral and the energy integral) which is mainly determined by how far the atomic wave function decays away from atomic site τ_i to atomic site $\mathbf{R}+\tau_j$. If $\mathbf{R}$ is very remote from site τ_i, which corresponds to the zeroth lattice site, the atomic wave-function overlap is insignificant. Therefore, there is a natural spatial cutoff, R_c, in the sum $\sum_{\mathbf{R}}$ in Eq. (4), beyond which the probability amplitude of electron hopping from site $\mathbf{R}+\tau_j$ to the zeroth lattice site is negligible. Such a locality property, namely, that electrons at remote sites do not interact, will be fully exploited and the numerical value for R_c with reference to the local-pseudopotential Hamiltonian will be presented in later discussion. Another important aspect of Eq. (4a) is that $g_{\alpha\beta}^{ij}(\mathbf{R})$ depends mainly on $\mathbf{R}$ and is independent of the momentum $\mathbf{k}$ in contrast with a similar equation [cf. Ref. 6, Eq. (7)] in the momentum representation. Therefore, once the g functions are known, the Hamiltonian matrix elements at any momentum $\mathbf{k}$ can be evaluated simply by summing over the g functions multiplied by a phase factor $e^{i\mathbf{k}\cdot\mathbf{R}}$ at each site $\mathbf{R}$ lying within a radius R_c. This spatial Fourier series analysis indicates that this tight-binding formulation can be developed into an efficient band-structure–calculation algorithm from a computational viewpoint. Furthermore, it implies that a complete description of the band structure requires all neighbor interactions of a cluster of atoms in a volume of $4\pi R_c^3/3$ inside the crystal. In the next section, we present an in-depth discussion and explicit expressions of this formalism with reference to the local-pseudopotential Hamiltonian.

III. LOCAL-PSEUDOPOTENTIAL HAMILTONIAN

The local pseudopotential is defined as

$$V(\mathbf{r})\equiv\sum_{\mathbf{G}} e^{i\mathbf{G}\cdot\mathbf{r}} v(\mathbf{g})\ , \tag{5}$$

where $\mathbf{G}$ is the reciprocal-lattice vector and $v(\mathbf{G})$ is the form factor given by

$$v(\mathbf{G})=v_s(\mathbf{G})\cos(\mathbf{G}\cdot\boldsymbol{\tau})-iv_a(\mathbf{G})\sin(\mathbf{G}\cdot\boldsymbol{\tau})\ .$$

We use Cohen and Bergstresser[12] parameters for v_s and

v_a. The displacement vector τ is $(1,1,1)(a/8)$. The sum in Eq. (5) is limited to all G's which lie within a radius of $\sqrt{11}(2\pi/a)$ where a is the lattice constant. The full single-particle Hamiltonian is $H=p^2/2m+V(\mathbf{r})$. The eigenvalue problem of finding the band energy is equivalent to finding the roots of the equation $\det(H-ES)=0$ in the Bloch basis. By use of Eq. 4(a), the matrix elements for the kinetic energy are

$$\left\langle \phi_\alpha^i(\mathbf{k},\mathbf{r}) \left| \frac{\mathbf{p}^2}{2m} \right| \phi_\beta^j(\mathbf{k},\mathbf{r}) \right\rangle = -\frac{N\hbar^2}{2m} \sum_{\mathbf{R}} e^{i\mathbf{k}\cdot\mathbf{R}} [P^x_{0i\alpha;\mathbf{R}j\beta} F^y_{0i\alpha;\mathbf{R}j\beta}(0) F^z_{0i\alpha;\mathbf{R}j\beta}(0) + F^x_{0i\alpha;\mathbf{R}j\beta}(0) P^y_{0i\alpha;\mathbf{R}j\beta} F^z_{0i\alpha;\mathbf{R}j\beta}(0) + F^x_{0i\alpha;\mathbf{R}j\beta}(0) F^y_{0i\alpha;\mathbf{R}j\beta}(0) P^z_{0i\alpha;\mathbf{R}j\beta}] . \quad (6)$$

The matrix elements for the potential energy, Eq. (5), are

$$\langle \phi_\alpha^i(\mathbf{k},\mathbf{r}) | V(\mathbf{r}) | \phi_\beta^j(\mathbf{k},\mathbf{r}) \rangle = N \sum_{\mathbf{R}} e^{i\mathbf{k}\cdot\mathbf{R}} \left[\sum_{\mathbf{G}} v(\mathbf{G}) F^x_{0i\alpha;\mathbf{R}j\beta}(\mathbf{G}) F^y_{0i\alpha;\mathbf{R}j\beta}(\mathbf{G}) F^z_{0i\alpha;\mathbf{R}j\beta}(\mathbf{G}) \right] . \quad (7)$$

The matrix elements for the overlap integral are

$$\langle \phi_\alpha^i(\mathbf{k},\mathbf{r}) | \phi_\beta^j(\mathbf{k},\mathbf{r}) \rangle = N \sum_{\mathbf{R}} e^{i\mathbf{k}\cdot\mathbf{R}} F^x_{0i\alpha;\mathbf{R}j\beta}(0) F^y_{0i\alpha;\mathbf{R}j\beta}(0) F^z_{0i\alpha;\mathbf{R}j\beta}(0) . \quad (8)$$

In these equations,

$$F^x_{0i\alpha;\mathbf{R}j\beta}(\mathbf{G}) \equiv \int dx\, e^{-2(\lambda_i+\lambda_j)x^2+ixG_x} Q^x_\alpha Q^x_\beta \quad (9)$$

and

$$P^x_{0i\alpha;\mathbf{R}j\beta} \equiv \int dx\, e^{-\lambda_i x^2} Q^x_\alpha \frac{\partial^2}{\partial x^2} (Q^x_\beta e^{\lambda_j x^2}) , \quad (10)$$

where Q^x_α is defined as the x factor in the polynomial of the Gaussian wave function f_α. For example, for the s Gaussian orbital, $Q^x_{\alpha=s}=1$, and for the p_y Gaussian orbital, $Q^y_{\alpha=p_y}=y$, and so forth. By using the Fourier transform, one can build up the F's and P's of all Gaussian wave functions from the s-state wave function by two simple recurrence relations. Below we show how this can be done and discuss the physical implications of these relations.

A general Gaussian wave function is a product of a polynomial in x, y, and z with a Gaussian function $e^{-\lambda r^2}$, which can always be decomposible into $e^{-\lambda x^2} e^{-\lambda y^2} e^{-\lambda z^2}$. When an inner product is constructed as in Eqs. (6)–(8), term-by-term multiplication of the polynomials from the bra and ket produces terms of the form $x^m y^n z^l$ which are multiplied by the Gaussian functions of the x, y, and z components. Subsequent integration with respect to $\mathbf{r}$ can be done separately for each coordinate in the x, y,and z directions. Therefore, without loss of generality, we confine our derivation to the x component only. In general, the following function is encountered formally:

$$\omega_{nm}(g) \equiv \int dx\, (x-A)^n (x-B)^m e^{-\lambda_1(x-A)^2-\lambda_2(x-B)^2+igx} \quad (11)$$

where λ_1 and λ_2 are arbitrary real constants. A and B are the x component of τ_i and $\mathbf{R}+\tau_j$ in Eq. (4b), respectively. This function can be evaluated in closed form. The best approach is to consider the following integral:

$$h_r(g) \equiv \int dx\, x^r e^{-\lambda_1(x-A)^2-\lambda_2(x-B)^2+igx} = \left[-i\frac{\partial}{\partial g} \right]^r \omega_{00}$$

with

$$\omega_{00} = \left[\frac{\pi}{\lambda} \right]^{1/2} e^{-\lambda_1\lambda_2 U^2/\lambda + iDg - g^2/4\lambda} , \quad U \equiv A-B, \quad \lambda \equiv \lambda_1+\lambda_2, \quad D \equiv \frac{\lambda_1 A+\lambda_2 B}{\lambda} . \quad (12)$$

Defining $F^{(0)} \equiv \omega_{00}$, we immediately obtain the following useful recurrence relation:

$$F^{(l)} \equiv \left[-i\frac{\partial}{\partial g} \right]^l F^{(0)} = -iF^{(l-1)} \left[iD - \frac{g}{2\lambda} \right] + \frac{l-1}{2\lambda} F^{(l-2)} . \quad (13)$$

Therefore, Eq. (11) becomes

$$\omega_{nm}(g) = \sum_{k=0}^{n} \sum_{l=0}^{m} \binom{n}{k} \binom{m}{l} (-A)^{n-k} (-B)^{m-l} F^{(k+l)} . \quad (14)$$

Furthermore, a second recurrence relation related to the kinetic energy in Eq. (10) is obtained as follows. Define

$$P_{nm} \equiv \int dx\, (x-A)^n e^{-\lambda_1(x-A)^2} \frac{\partial^2}{\partial x^2} \times [(x-B)^m e^{-\lambda_2(x-B)^2}] .$$

Then,

$$P_{nm} = m(m-1)\omega_{nm-2} - 2\lambda_2(2m+1)\omega_{nm} + 4\lambda_2^2 \omega_{nm+2} . \quad (15)$$

The recurrence relations in Eqs. (13) and (15) show that the exponential factor $e^{-\lambda_1\lambda_2 u^2/\lambda}$ in Eq. (12) is the crucial factor that determines the magnitude of the $F^x_{0i\alpha;\mathbf{R}j\beta}(\mathbf{G})$ and $P^x_{0i\alpha;\mathbf{R}j\beta}$ contributing to the Hamiltonian matrix with respect to the variation of the relative distance U of two lattice points. It is a measure of the correlation of the two Gaussian atomic wave functions separated by a dis-

tance of U from each other. The exponential decay implies that if $U \gg (\lambda/\lambda_1\lambda_2)^{1/2}$, $F^x_{0i\alpha;\mathbf{R}j\beta}(\mathbf{G})$'s and $P^x_{0i\alpha;\mathbf{R}j\beta}$'s contributions are negligible. This forms the theoretical basis of the spatial truncation in our numerical works. In practice, for the minimal basis set of sp^3 Gaussian orbitals, the spatial truncation is defined by R_c with a numerical value of at least $4(\lambda/\lambda_1\lambda_2)^{1/2}$ which is defined as the spatial correlation factor. This factor determines the minimal number of near-neighbor interactions measured from the center of a cluster of primitive cells of size $(256\pi/3)(\lambda/\lambda_1\lambda_2)^{3/2}$. These complete the analysis of the local-pseudopotential Hamiltonian.

IV. NUMERICAL RESULTS

In this numerical works, we employed Chen and Sher's optimal values[7] for λ_1 $(=0.352\pi/a^2)$ and λ_2 $(=0.212\pi/a^2)$. These parameters mean that the spatial correlation factor $4(\lambda/\lambda_1\lambda_2)^{1/2}$ is about $1.75a$, corresponding to a cluster of 87 primitive cells. We used a to denote the lattice constant of GaAs. To study the change of the band structure with respect to the variation of the spatial cutoff, we evaluated the band energies with different spatial cutoff values from $R_c=0.433a$, the nearest neighbor, to $R_c^{\min}$, a cutoff value that gives a convergence error of better than 0.05%. $R_c^{\min}$ is found to be $2a$ (Table I). Table II is a comparison of the band energies for the plane-wave (PW) basis and the Gaussian basis in the momentum (GOM) and the spatial (GOS) representations. It indicates that band structures of GOS (i.e., this method with a spatial truncation of $R_c=2a$) and GOM (i.e., Chadi's method in Ref. 6) are almost identical and compare very well with PW. Table III presents the energy integrals of the empirical pseudopotential up to second-nearest neighbors. Note that the local pseudopotential is not spherical. This gives rise to nonzero contributions to $E_{XY}(011)_C$, $E_{XY}(011)_A$, $E_{SX}(011)_C$, and $E_{SX}(011)_A$ which have zero-overlap integrals. Note also that $E_{XX}(000)_A$ and $E_{XX}(000)_C$ contribute significantly more to the Hamiltonian matrix, in contrast with earlier results[13,14] obtained by adjusting directly the tight-binding parameters. The overall characteristic of the energy integrals is that they do not decrease rapidly with increase in distance. Figures 1(a) and 1(b) show that the nearest- and second-nearest-neighbor interactions with the energy integrals defined in Table III cannot account the band structure of the local pseudopotential. Their band structures are completely different from the bulk band structure and from each other. Even their valence bands are not the same. The band structures become similar to the local-pseudopotential band structure only for sufficiently large $R_c > 1.58a$. Figure 2 shows the band structure at $R_c=1.41a$ which appears better than that of the nearest- and second-nearest-neighbor interactions. The high-lying conduction bands push down at the Γ point. The shapes of the valence bands and the first conduction band are similar, but their values are by no means close to that of the plane-wave basis. Furthermore, the band gap at the Γ point is too small though it predicts a direct band gap. As the cutoff increases, the band structure steadily improves and finally converges to

TABLE I. Band energies (eV) for different spatial cutoffs. The number in square brackets [ ] is the degeneracy. N_c is the number of primitive cells in a cluster with a spatial radius of R_c.

	$R_c=1.6a$ $N_c=79$	$R_c=1.84a$ $N_c=87$	$R_c=1.95a$ $N_c=135$	$R_c=2.0a$ $N_c=141$
Γ_{1v}	−12.802	−12.679	−12.591	−12.591
Γ_{15v}	0.0	0.0	0.0 [3]	0.0 [3]
	−0.219 [2]	−0.081 [2]		
Γ_{1c}	1.143	1.309	1.417	1.417
Γ_{15c}	3.704	4.097	4.416 [3]	4.418 [3]
	4.047 [2]	4.226 [2]		
X_{1v}	−10.760	−10.638	−10.550	−10.550
X_{3v}	−6.163	−6.039	−5.951	−5.951
X_{5v}	−2.394 [2]	−2.268 [2]	−2.183 [2]	−2.183 [2]
X_{1c}	1.679	1.778	1.871	1.871
X_{3c}	1.984	2.016	2.121	2.121
L_{1v}	−11.345	−11.221	−11.132	−11.132
L_{2v}	−6.447	−6.343	−6.270	−6.270
L_{3v}	−0.929 [2]	−0.806 [2]	−0.719 [2]	−0.719 [2]
L_{1c}	1.127	1.378	1.540	1.540
L_{3c}	5.033 [2]	5.040 [2]	5.167 [2]	5.168 [2]

TABLE II. Band energies of GaAs (eV) calculated using 89 plane waves (PW), the Gaussian orbital in momentum representation (GOM), and the Gaussian orbital in spatial representation (GOS) with $R_c=2a$.

	PW	GOM	GOS
Γ_{1v}	−12.22	−12.54	−12.59
Γ_{15v}	0.0	0.0	0.0
Γ_{1c}	1.42	1.42	1.42
Γ_{15c}	4.43	4.42	4.42
X_{1v}	−10.14	−10.51	−10.55
X_{3v}	−6.09	−5.91	−5.95
X_{5v}	−2.23	−2.11	−2.18
X_{1c}	1.77	1.90	1.87
X_{3c}	2.09	2.13	2.12
L_{1v}	−10.75	−11.08	−11.13
L_{2v}	−5.96	−6.15	−6.27
L_{3v}	−0.89	−0.71	−0.72
L_{1c}	1.69	1.53	1.54
L_{3c}	4.96	5.17	5.17

TABLE III. The local-pseudopotential nearest-neighbor and second-nearest-neighbor energy integrals (eV) for GaAs. A and C stand for anion and cation, respectively.

$[E_{SS}(000)]_C$	−1.355	$[E_{SS}(000)]_A$	1.924
$[E_{XX}(000)]_C$	6.278	$[E_{XX}(000)]_A$	4.931
$E_{SS}(\frac{1}{2}\frac{1}{2}\frac{1}{2})$	−0.659	$[E_{SX}(\frac{1}{2}\frac{1}{2}\frac{1}{2})]_{CA}$	0.202
$[E_{SX}(\frac{1}{2}\frac{1}{2}\frac{1}{2})]_{AC}$	0.697	$E_{XX}(\frac{1}{2}\frac{1}{2}\frac{1}{2})$	0.358
$E_{XY}(\frac{1}{2}\frac{1}{2}\frac{1}{2})$	−1.484	$[E_{XY}(110)]_C$	−0.181
$[E_{XY}(011)]_C$	0.152	$[E_{XY}(110)]_A$	−0.928
$[E_{XY}(011)]_A$	−0.542	$[E_{XX}(110)]_C$	−0.168
$[E_{XX}(110)]_A$	−0.539	$[E_{XX}(011)]_C$	−0.055
$[E_{XX}(011)]_A$	0.020	$[E_{SX}(110)]_C$	0.168
$[E_{SX}(011)]_C$	−0.082	$[E_{SX}(110)]_A$	−0.130
$[E_{SX}(011)]_A$	0.376	$[E_{SS}(110)]_C$	−0.195
$[E_{SS}(110)]_A$	−0.159		

Fig. 4. Figure 3 shows the band structure at $R_c = 1.6a$, which is very close to the local-pseudopotential band structure. These results strongly indicate that intermediate-range interactions within a spatial extent of about $2.0a$ are important in the local-pseudopotential Hamiltonian system. This also suggests that the intermediate-range interactions are important in the nonlocal-pseudopotential Hamiltonian system since it in-

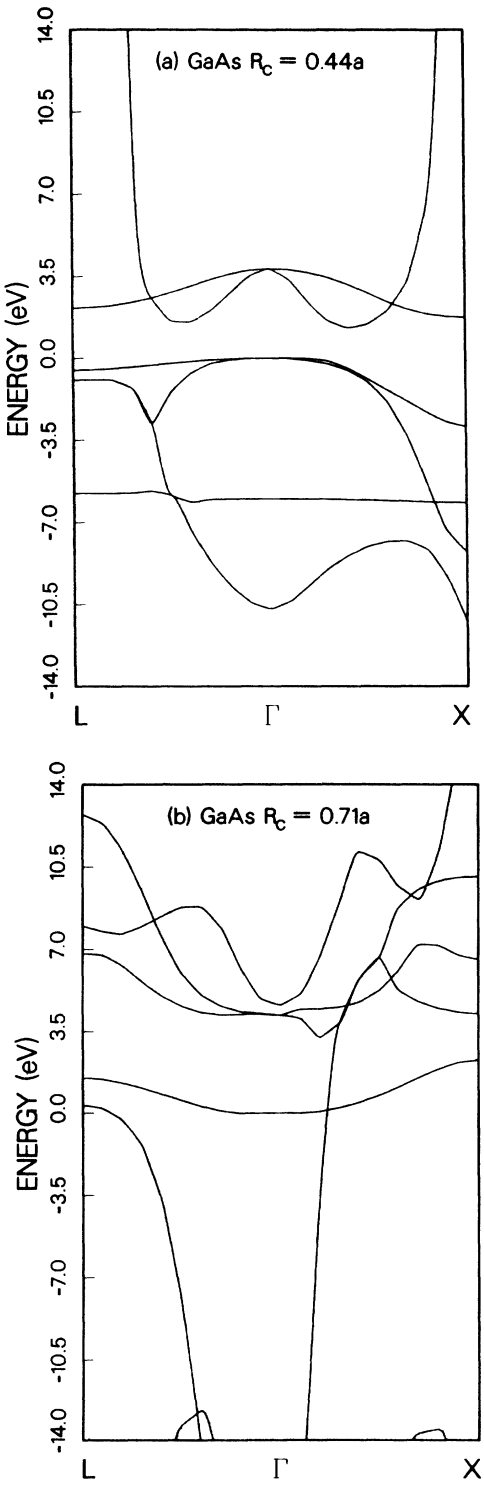

FIG. 1. The band structures of GaAs calculated using (a) the nearest-neighbor interaction of the local pseudopotential with a cutoff of $R_c = 0.44a$, and (b) the nearest- and second-nearest-neighbor interactions of the local pseudopotential with a cutoff of $R_c = 0.71a$.

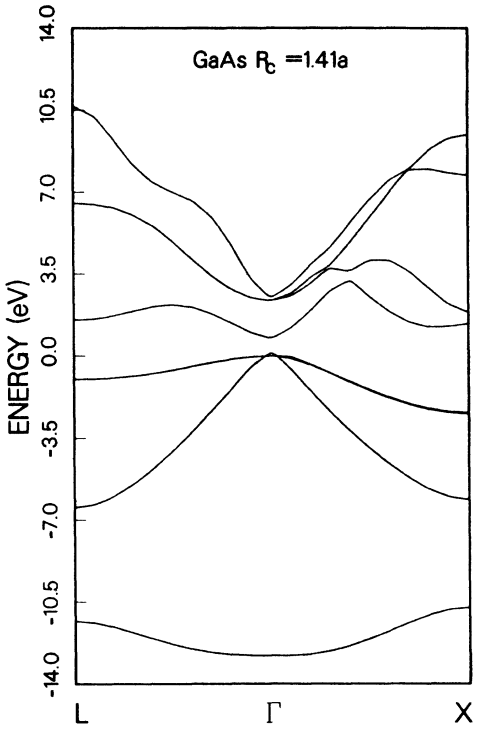

FIG. 2. The band structure of GaAs calculated using the spatial tight-binding theory with a cutoff of $R_c = 1.41a$.

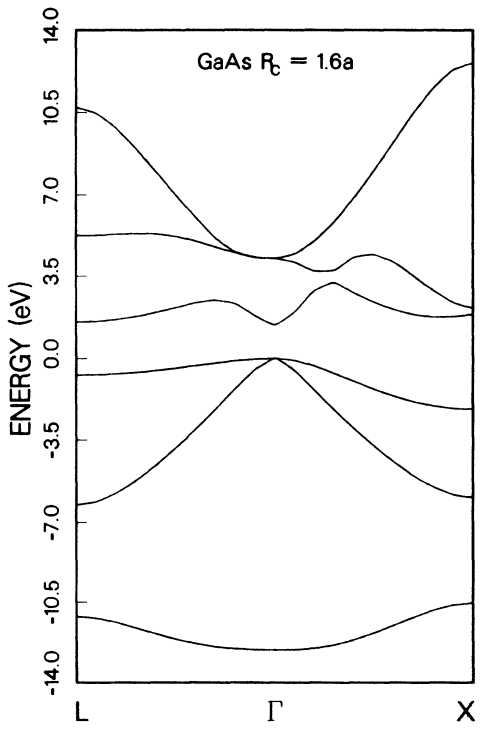

FIG. 3. The band structure of GaAs calculated using the spatial tight-binding theory with a cutoff of $R_c = 1.6a$.

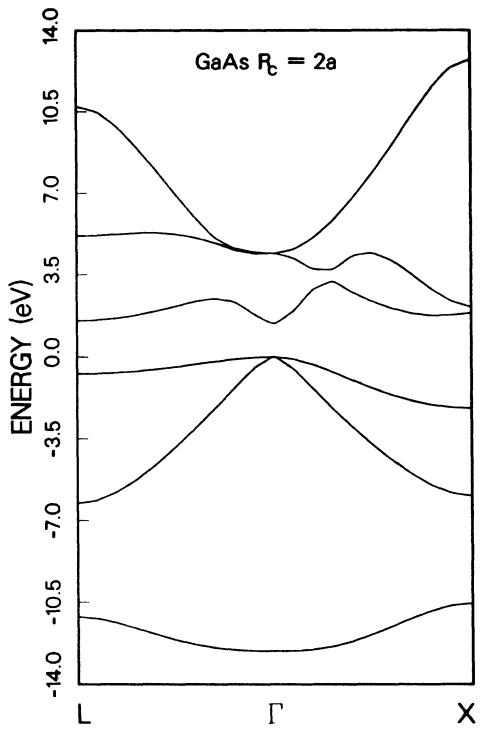

FIG. 4. The band structure of GaAs calculated using the spatial tight-binding theory with a cutoff of $R_c = 2a$.

cludes the local-pseudopotential Hamiltonian in addition to the nonlocal piece and the spin-orbit interactions.

V. CONCLUSIONS

We have presented in this paper a complete treatment of the local-pseudopotential Hamiltonian by the tight-binding theory in the spatial representation. We have demonstrated that good agreements with the band structure obtained via the plane-wave basis can be obtained if the lattice cutoff is sufficiently large. Convergence to better than 0.05% can be attained if the cutoff is about $1.85a$ (number of neighbor lattice sites of 135) and beyond for GaAs. This study shows that the tight-binding theory when properly formulated produces reliable results which are based on a few adjustable form factors in the momentum space. This study also shows that intermediate-range interactions are important and has to be included in the tight-binding theory so to properly account for the full local-pseudopotential band structure. This study brings out a deeper relation of the tight-binding theory with the pseudopotential Hamiltonian system and also indicates to some degree the potential application of the present formalism to nonlocal-pseudopotential Hamiltonians and more complicated structures involving defects, heterojunctions, and microstructures.

ACKNOWLEDGMENTS

This work was supported by The Texas Advanced Technology Research Program and the Robert A. Welch Foundation.

[1]J. C. Slater and G. F. Koster, Phys. Rev. **94**, 1498 (1954); W. A. Harrison, *Electronic Structure and the Properties of Solids* (Freeman, San Francisco, 1980).

[2]D. J. Chadi and M. L. Cohen, Phys. Status Solidi **68**, 405 (1975).

[3]R. P. Messer, Chem. Phys. Lett. **11**, 589 (1971); M. Nishida, J. Chem. Phys. **69**, 956 (1978); R. Hoffmann, *ibid.* **39**, 1397 (1963).

[4]N. Sahu, J. T. Borenstein, V. A. Singh, and J. W. Corbett, Phys. Status Solidi. B **122**, 661 (1984).

[5]P. Vogl, H. P. Hjalmarson, and J. D. Dow, J. Phys. Chem. Solids **44**, 365 (1983).

[6]D. J. Chadi, Phys. Rev. B **16**, 3572 (1977).

[7]A. B. Chen and A. Sher, Phys. Rev. B **22**, 3886 (1980); **26**, 6603 (1982).

[8]E. E. Lafon and C. C. Lin, Phys. Rev. **152**, 579 (1966); R. C. Chanery, T. K. Tung, C. C. Lin, and E. E. Lafon, J. Chem. Phys. **52**, 361 (1970); R. C. Chaney, C. C. Lin, and E. E. Lafon, Phys. Rev. B **3**, 459 (1971); R. C. Chaney, E. E. Lafon, and C. C. Lin, *ibid.* **4**, 2734 (1971); J. E. Simmons, C. C. Lin, D. F. Fouquet, E. E. Lafon, and R. C. Chaney, J. Phys. C **8**, 1549 (1975).

[9]E. O. Kane, Phys. Rev. B **13**, 3478 (1976).

[10]S. Ciraci, J. Phys. Chem. Solids **36**, 557 (1975); S. Ciraci and I. P. Batra, Phys. Rev. B **15**, 3254 (1977); *ibid.* **15**, 4923 (1977); I. P. Batra, J. Vac. Sci. Technol. **16**, 1359 (1979).

[11]C. S. Wang and B. M. Klein, Phys. Rev. **24**, 3393 (1981).

[12]M. L. Cohen and T. K. Bergstresser, Phys. Rev. **141**, 789 (1966).

[13]S. Nara, Jpn. J. Appl. Phys. **26**, 690 (1987).

[14]G. C. Osbourn and D. L. Smith, Phys. Rev. B **19**, 2124 (1979).